

OPTICAL AND SURFACE CHARACTERIZATION OF ALKALI-ANTIMONIDE PHOTOCATHODES

P. Saha*, O. Chubenko, G. S. Gevorkyan, A. H. Kachwala, S. S. Karkare, C. J. Knill
Arizona State University, Tempe, AZ, USA

H. A. Padmore, Lawrence Berkeley National Laboratory, Berkeley, CA, USA

E. J. Montgomery, S. Poddar, Euclid Beamlabs LLC, Gaithersburg, MD, USA

Abstract

Alkali-antimonides, characterized by high quantum efficiency and low mean transverse energy in visible light, are excellent electron sources to drive x-ray free electron lasers, electron cooling and ultrafast electron diffraction applications etc. Existing studies of alkali-antimonides have focused on quantum efficiency and emittance, but information is lacking on the fundamental aspects of the electronic structure, such as the energy gap of the semiconductor and the density of defects as well as the overall nano-structure of the materials. We are, therefore, conducting photoconductivity measurements to measure fundamental semiconductor properties as well as using atomic force microscope (AFM) and kelvin probe force microscope (KPFM) to measure the nanostructure variations in structure and surface potential.

INTRODUCTION

Alkali-antimonides are an interesting class of semiconductors that have emerged as promising candidates for photoemission-based electron sources for next generation x-ray free electron lasers, ultrafast electron diffraction and electron-beam based hadron cooling applications due to their extremely high quantum efficiency (QE) compared to metal cathodes and a relatively low intrinsic emittance, or mean transverse energy (MTE), in the visible wavelengths [1]. Increasing the QE to its highest possible value to mitigate the non-linear photoemission effects and simultaneously reducing the MTE to the smallest possible value, is critical for obtaining the smallest possible emittance and the brightest possible electron beam from photoinjectors used for the above applications [1].

Alkali-antimonide materials have been well characterized in terms of their photoemission properties like QE and MTE. However, very little is known about their semiconducting properties like the energy band-gap and density of states. Such knowledge is critical for obtaining a deep understanding of the photoemission process and developing alkali-antimonide materials and their heterostructures which exhibit higher QE and lower MTEs [2].

It has been demonstrated that the MTE from alkali-antimonide photocathodes can be significantly reduced by operating them at near-threshold wavelengths and cooling them down to cryogenic temperatures [3]. However, the thermal limit of MTE [4] has still not been achieved from alkali-antimonides. One of the reasons for the increased

MTE is the surface non-uniformities like physical roughness and work-function variations [5]. Such variations result from the nature of the deposition process used to grow the alkali-antimonide thin films [6]. Ultra-smooth surfaces of Cs-Sb cathodes are required in order to attain the thermal limit to the MTE from these cathodes [6].

In this paper, we report on the synthesis of several Cs-Sb cathodes, grown on different substrates using the co-deposition process [6]. We perform spectrally-resolved photoconductivity measurements to study the properties of electronic structure of these films. We also study the surface morphology and work function variations of these cathodes under ultra high vacuum-atomic force microscope/kelvin probe force microscope (UHV-AFM/KPFM) [7], and try to find the factors which contribute to the roughness of films. We demonstrate the growth of atomically smooth alkali-antimonide films, which can minimize the surface non-uniformities contribution to the MTE.

GROWTH PROCESS

Several Cs-Sb cathodes were grown on 10 mm by 10 mm p-type Si (100), fused silica, and Nb-doped strontium titanate (STO) substrates using the co-deposition technique [6]. The 0.5 mm thick substrates were rinsed with isopropyl alcohol and annealed at 600 °C for 2 hours before growth. This results in a disordered surface for amorphous fused silica substrates and Si substrates with native oxide layers. However, this generates a well-ordered, atomically clean surface for STO. The ordered surface of STO substrates was confirmed by observing the atomic terraces on the surface, using an UHV-AFM connected in vacuum to the growth/preparation chamber.

The UHV growth chamber has a base pressure in the low 10^{-10} Torr range. Sb and Cs are evaporated simultaneously by heating 99.9999 % pure Sb pellets obtained from Alfa Aesar [8] and cesium molybdate pellets obtained from SAES Getters [9], in their respective effusion cells. The substrate holder is negatively biased to 30-35 V to collect the photocurrent emitted from the cathode, in order to measure the QE during and after the deposition process.

During the deposition, the Sb source temperature is maintained at 400 °C, which corresponds to a flux rate of 0.01 A°/s pre-calibrated with a quartz crystal balance. Cs source temperature is in the range of 350-450 °C to obtain a Cs partial pressure of $\sim 1.2 \times 10^{-10}$ torr, on the RGA. The Cs partial pressure slowly changes with time at a particular source temperature as the source depletes. We gradually increase the

* psaha6@asu.edu

Content from this work may be used under the terms of the CC BY 3.0 licence (© 2021). Any distribution of this work must maintain attribution to the author(s), title of the work, publisher, and DOI

temperature to maintain the Cs partial pressure. The rate at which Cs partial pressure changes during growth is small enough that we do not need to vary the Cs deposition temperature significantly during one growth. All the growths were performed at a substrate temperature of 75 °C.

The photocurrent emitted by the cathode under illumination of a 532 nm laser is monitored to obtain the QE during the growth. When the QE begins to saturate, growth is terminated by cooling down both the sources simultaneously. The substrate heater is also turned off, which allows a gradual cooling of the substrate to room temperature. All the Cs-Sb cathodes yielded a final QE between 3-5 % at 532 nm.

CATHODE CHARACTERIZATION

QE Spectral Response

The QE spectral response of Cs-Sb photocathodes is measured using an Optical Parametric Amplifier (OPA) — in this case a Light Conversion Orpheus pumped by the Light Conversion Pharos [10]. Figure 1(a) shows the spectral response of Cs-Sb photocathodes grown on STO, Si and fused silica substrates, by co-deposition technique. The cathodes grown on different substrates have identical photoemission threshold and comparable QE.

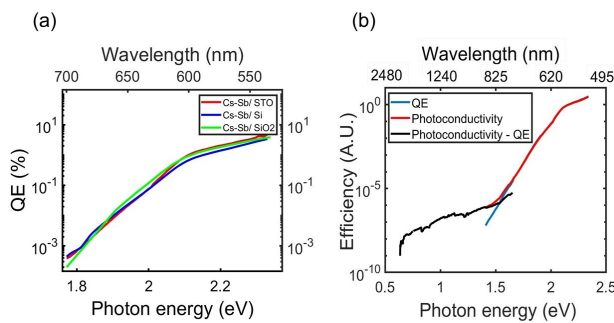


Figure 1: (a) Comparison of QE spectral response of Cs-Sb photocathodes grown on STO, Si and fused silica substrates, and (b) Plot of PC efficiency of Cs-Sb/SiO₂ vs incident photon energy.

Photoconductivity (PC) Measurement

Photoconductivity measurements require an insulating substrate and hence was performed on films grown on fused silica. A thin 100 nm layer of platinum (Pt) was deposited via evaporation on the 10 mm × 10 mm fused silica substrate on selected regions of dimensions: length = 3 mm, width = 2 mm, to serve as contacts for PC measurements. Prior to the Pt deposition, a very thin 10 nm layer of titanium was deposited on these regions of the substrate for adhesion of Pt to fused SiO₂. Spectrally resolved PC response is measured by shining light from the OPA, modulated with a mechanical chopper, on Cs-Sb/SiO₂, and recording the photo-induced current across the film with a lock-in amplifier when a bias of 33 V is applied across the two Pt contacts.

Neutral density filters are used as required to prevent non-linear optical processes like multiphoton absorption/emis-

sion. The laser spot covered a large area of the sample surface area to minimize the effect of such non-linear processes.

Figure 1(b) shows our measurements of PC response from Cs-Sb/SiO₂ at photon energies between 0.6-2.4 eV, corresponding to wavelengths between 1950-500 nm, at room temperature. The efficiency is calculated by normalizing the photo-induced current at different wavelengths, by the number of incident photons per second. The PC response, as indicated by the red curve in Fig. 1(b), is obtained by applying a positive voltage of 33 V across the gap between the electrodes, while the QE spectral response is obtained as discussed in the previous section. It can be observed that at photon energies slightly below and beyond the photoemission threshold (above 1.6 eV), PC efficiency (red curve) and QE response (blue curve) are barely distinguishable from one another. This could be explained by photoemission of electrons from the conduction band of Cs-Sb into vacuum, by overcoming the work function of the material at these higher photon energies (close to and above the threshold). These emitted electrons move towards the positive contact in vacuum, thereby constituting the photoemission response (QE). Pure PC response/ behavior can be obtained, by subtracting the QE from PC efficiency data (black curve), below photon energies of 1.6 eV. From the PC experimental data, the band gap can be deduced as the value of photon energy at which photoconductivity efficiency stops rising sharply with photon energy [11]. An order of magnitude rise of this sort strongly indicates the band gap energy of Cs-Sb photocathodes to be around 0.65 eV.

Surface Non-Uniformities

The surface morphology and work-function variations of different Cs-Sb photocathodes, are studied in vacuum using a RHK UHV-AFM/KPFM, connected to the growth chamber.

Cathodes grown on different substrates (STO and Si) are compared and contrasted in terms of their surface roughness. The commercially available substrates have atomically flat surfaces, with sub 0.3 nm rms roughness. After growth and spectral response measurements, the cathodes are transferred in UHV, into the UHV-AFM.

Figures 2(a) and 2(b) show the 2D topography maps of two Cs-Sb films grown on doped STO substrate, for 20 minutes and 1.5 hours, respectively. It can be seen that the cathode deposited for a shorter period of time, has a lower rms roughness amplitude of 0.31 nm and the average spacing between neighboring peaks is ~ 60 nm. The cathode grown by deposition over 1.5 hrs, has a larger roughness amplitude of 0.57 nm rms, with nearest neighbor peaks spaced at ~ 100 nm apart.

Figures 2(c) and 2(d) show the AFM images of two Cs-Sb cathodes grown on Si substrate, for 35 minutes and 1 hour 20 minutes, respectively. The film grown over a shorter period of time is much smoother with a roughness amplitude of 0.32 nm rms, and neighboring peak spacing of ~ 30 nm. On the other hand, the film grown over a longer

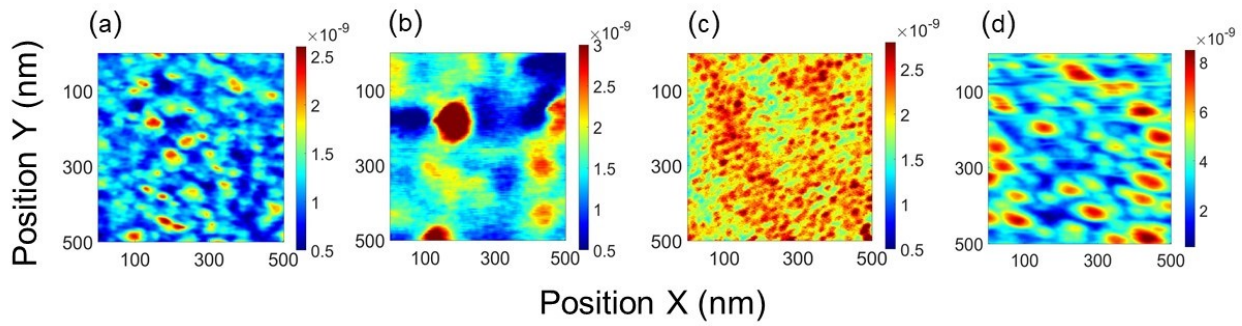


Figure 2: AFM images of Cs-Sb photocathodes grown on: (a) STO for 20 minutes, (b) STO for 1.5 hours, (c) Si for 35 minutes, and (d) Si for 1 hour and 20 minutes.

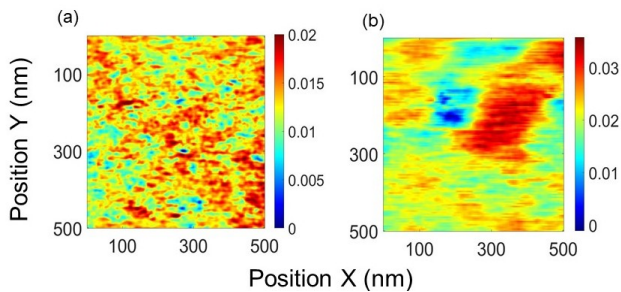


Figure 3: KPFM images of Cs-Sb photocathodes grown on STO substrate for (a) 20 minutes, and (b) 1.5 hours.

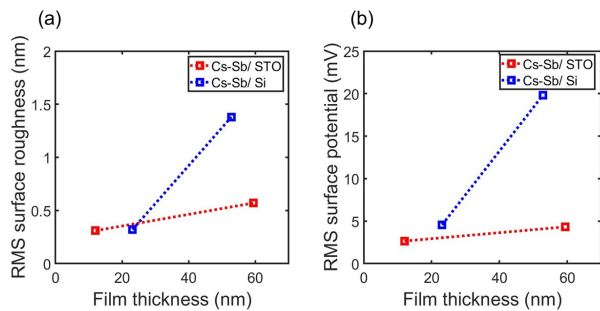


Figure 4: Surface roughness of different Cs-Sb photocathodes measured as a function of film thickness: (a) height variation/physical roughness, and (b) work function variation/chemical roughness.

period of time, has a significantly larger roughness amplitude of 1.38 nm rms, with an inter-neighbor peak distance of ~ 100 nm.

Figures 3(a) and 3(b) show the comparison between KPFM images of the two Cs-Sb films grown on doped STO (reported earlier in Fig. 2(a) and 2(b)). It can be seen that the amplitude of surface potential variation of cathode grown for 20 minutes (Fig. 3(a)) is lower. The average rms surface work function is 2.65 mV, with nearest neighbors spaced ~ 60 nm apart, whereas the rms surface work function of Cs-Sb/STO grown for 1.5 hours (Fig. 3(b)) is 4.32 mV, and the nearest neighbor spacing is ~ 100 nm.

Figure 4 shows the effect of film thickness and choice of substrate, on the surface roughness of the different Cs-Sb photocathodes discussed above. The film thickness was approximately calculated by multiplying the cesium and antimony flux rates, during growth, with time of co-deposition. It can be seen that both physical and chemical roughness of the Cs-Sb films on a particular substrate, are directly proportional to the film thickness: the thicker the film is, the rougher the surfaces are. The roughness amplitudes are not too different for films of varying thickness grown on doped STO substrates. However, the effect is dramatic in case of Cs-Sb/Si films, where the thicker film has an amplitude of physical roughness three times larger than the film with lower thickness. This is indicated by the blue curves in Fig. 4, whose slopes are much higher than that of the corresponding red curves for Cs-Sb/STO cathodes.

The roughness contribution to the MTE from the smooth Cs-Sb cathodes is calculated to be <1.0 meV for a wide range of electric fields typically used in photoinjectors [12, 13].

CONCLUSION AND FUTURE WORK

Based on our photoconductivity measurements, we have predicted the band gap energy of Cs-Sb photocathodes to be around 0.65 eV. We have demonstrated the growth of high QE Cs-Sb photocathodes, with sub-nm physical roughness and ultra-smooth chemical roughness. Simulations of the contribution of roughness to MTE from these cathodes, indicate highly promising performance, in low emittance applications.

Further work is underway to: (i) to perform photoconductivity studies on films grown on different substrates under different growth conditions, and (ii) to measure the effect of different growth conditions (fluxes and substrate temperature) on the surface non-uniformities of the cathodes.

ACKNOWLEDGEMENTS

This work was supported by the U.S. National Science Foundation under Award No. PHY-1549132 the Center for Bright Beams, the DOE under Grant No. DE-SC0021092, and Grant No. DE-SC0020575.

REFERENCES

- [1] P. Musumeci *et al.*, “Advances in bright electron sources”, *Nucl. Instrum. Meth. A.*, vol. 907, p. 209, 2018. doi:10.1016/j.nima.2018.03.019
- [2] P. Gupta, *et al.*, “Monte Carlo simulations of electron photoemission from cesium antimonide”, *J. Appl. Phys.*, vol. 121, p. 215702, 2017. doi:10.1063/1.4984263
- [3] L. Cultrera *et al.*, “Cold electron beams from cryocooled, alkali antimonide photocathodes”, *Phys.Rev. Spec. Top.-Accel. Beams.*, vol. 18, p. 113401, 2015. doi:10.1103/PhysRevSTAB.18.113401
- [4] J. Feng *et al.*, “Thermal limit to the intrinsic emittance from metal photocathodes”, *Rev. Sci. Instrum.*, vol. 86, p. 015103, 2015. doi:10.1063/1.4931976
- [5] S. Karkare and I. Bazarov, “Effect of nanoscale surface roughness on transverse energy spread from gaas photocathodes”, *Applied Physics Letters*, vol. 98, p. 094104, 2011. doi:10.1063/1.3559895.
- [6] J. Feng *et al.*, “Near atomically smooth alkali antimonide photocathode thin films”, *J. Appl. Phys.*, vol. 121, p. 044904, 2017. doi:10.1063/1.4974363.
- [7] UHV AFM, <http://www.rhk-tech.com/products/beetle-uhv-vt-afm/>.
- [8] Pure antimony metal, <https://www.alfa.com/en/>.
- [9] Cs pellets, <https://www.saesgetters.com/>.
- [10] OPA, <https://lightcon.com/>.
- [11] W. Spicer, “Photoemissive, Photoconductive, and Optical Absorption Studies of Alkali-Antimony Compounds”, *Phys. Rev.*, vol. 112, p. 114, 1958. doi:10.1103/PhysRev.112.114
- [12] G. S. Gevorkyan *et al.*, “Effects of physical and chemical surface roughness on the brightness of electron beams from photocathodes”, *Phys. Rev. Accel. Beams.*, vol. 21, p. 093401, 2018. doi:10.1103/PhysRevAccelBeams.21.093401.
- [13] E. J. Montgomery *et al.*, “Towards Ultra-Smooth Alkali Antimonide Photocathode Epitaxy”, presented at the 12th Int. Particle Accelerator Conf. (IPAC’21), Campinas, Brazil, May 2021, paper WEPAB169, this conference.